OPTOELECTRONICS AND ADVANCED MATERIALS – RAPID COMMUNICATIONS Vol. 9, No. 9-10, September – October 2015, p. 1143 - 1146

Metallic micro/nanowire arrays with largely tunable diameter and spacing: fabrication and application

NIU GAO[a,b], YANG BO[b], YANG YI[b], LIU XUDONG[b], YU BIN[b], ZHU YE[b], ZHOU XIUWEN[b,c,*]
[a]*Science and Technology on Plasma Physics Laboratory, Mianyang 621900, China*
[b]*Laser Fusion Research Center, China Academy of Engineering Physics, Mianyang 621900, China*
[c]*Sichuan University, Chengdu 610065, China*

The communication demonstrates an effective and simple method for mass production of metallic micro/nanowire arrays. The three dimensional geometric parameters of the metallic array can be tuned over a large range, from micron to nano-scale. Metallic micro/nanowire arrays with largely tunable diameter and spacing can be used to studying the interaction of intense femtosecond laser pulses with matter.

(Received August 24, 2015; accepted September 9, 2015)

Keywords: Micro/nanowire arrays, Laser targets, Polyethylene templates, Co-drawing

1. Introduction

The interaction between intense ultrashort pulse laser and solid targets have been of considerable interest because of the potential applications such as production of energetic electron or ion beams, [1–5] high-brightness X-ray or Kα sources, [6–8] high-order harmonics, [9] as well as in the fast ignition approach to inertial confinement fusion. [10] When a flat solid surface is irradiated by an intense ultrashort laser pulse, a high-conductivity plasma forms at the surface. [11,12] The ionization generated by the intense laser pulses creates a 'critical electron density' that limits the penetration of the light into the target, resulting in the laser energy being deposited in a thin surface layer (called skin depth) of the material with a low efficiency. As the plasma has a high refractive index, the peak reflectivity for visible and near-infrared wavelengths is greater than 90%. Consequently, the laser light is reflected by the mirror-like hot metal surface, and hence the absorption of the laser light is low. The structured solid surfaces of objects such as gold clusters, gratings, porous structures and nanowires can be used to enhance the absorption of the laser light. [11] The advantages of such structured targets include a higher energy deposition per unit volume and enhanced X-ray emission. One attractive way to increase the efficiency is introducing metal micro/nanowire arrays targets ("nanobrush" or "velvet" targets) which have low average density and high local density. Two dimensional (2D) particle-in-cell (PIC) simulation confirms that a nanowire arrays target can lead to enhanced laser energy absorption, as well as electron acceleration and collimation. [13] The major advantage of metal micro/nanowire arrays targets is that the nanowire fill-fraction can be altered to optimize absorption in the structure, but near-solid densities help to generate fast high intensity x-ray pulses from the laser plasma interaction. However, for metal micro/nanowire arrays laser targets applications, one important challenge that needs to be overcome is obtaining accurate control of the diameter, length, location, and packing manner of the micro/nanowires. [12] For example, metallic Cu (or other element) micro/nanowire arrays targets with largely tunable diameter (100nm~10μm), length (1μm~70μm), and spacing (0.1μm~30μm) are in dire need by the SILEX- Ⅰlaser facility of the Laser Fusion Research Center in Mianyang, China.

Much resarch effort has been devoted to the fabrication and applications of metallic micro/nanowires. [14–17] Template method is a simple and convenient method to fabricate metal nanowires and porous anodic aluminum oxide (AAO) is the most commonly used template. [18–25] The diameters and spacings of AAO pores are usually less than100nm, and it is difficult to exceed 400 nm, which limits its application to fabricate "nanobrush" or "velvet" targets. In this communication, we present a fabrication of Cu micro/nanowire arrays based on porous polyethylene (PE) templates with a high throughput by a convenient method. [26] The diameter and the center-to-center distance between nanowires have been accurately controlled in large scale. Finally, we investigated the interaction between intense ultrashort pulse laser and nanowire arrays solid targets. For comparison, Cu nanowire arrays solid target fabricated using the described technique and plane Cu were employed.

2. Experimental

The overall fabrication process of metallic micro/nanowire arrays is schematically depicted in Fig. 1. A PS rod was insetted into a PE tube and a preformed PE/PS composite rod was got. We carried out the size-reduction using a capillary rheometer which have a furnace with biggish entrance and lesser exit. The melt

co-drawing process was carried out at 2 mm/s drawing speed while feeding the preformed PE/PS composite rod at 0.08 mm/s into the furnace at 220 ℃. After this melt co-drawing process, the dumpy preformed PE/PS composite rod became to a gracile PE/PS composite fiber. The fiber obtained from the first drawing step was cut and arranged in hexagonal lattices inside a protective jacket (a thin-wall PE tube), vacuum consolidated and redrawn. [27] By repeating the draw-cut-stack process for two or three times, the PE/PS composite fibers embedded with ordered arrays of PS micro/nanowires were obtained. The diameters and spacings of the PS wires in PE matrix would decrease from millimeter to micron or nanometer. Whereafter, the PE/PS composite fiber was cut to segments with ~100 μm thickness. After dissolving PS fibers selectively in methylbenzene, we got a throughhole PE template with micro/nanohole arrays. Then, Cu film was deposited on one side of the template via megnetron sputtering in vacuum with the thickness about 1 mm at 1.3 $\times 10^4$ Pa and 40 W for 2 hr. A conducting wire was bonded on the Cu film to serve as an electrode. Then the sample was fixed on the quartz slide, the sample was covered with insulating tape and one side of the template was in exposure without Cu film. After this, the sample on the slide was dipped into electrolyte (solution of $CuSO_4$) and the electrodeposition was carried out at 1.4 V and 25 Hz DC pulse. After 6–7 min, the electrodeposition process was terminated. Then the sample was dipped into the 1,4-dimethylbenzene solution to be heated for dissolving PE template at about 150℃.

The experimental setup is shown in Fig. 3a. The laser can deliver energies up to 6 J (with a peak intensity of 7.9×10^{18} W cm^{-2}), the pulse duration is 31 fs, and the central wavelength is 800 nm. After entering the chamber, the *p*-polarized main laser is focused on the target with an *f* /3 off-axis-parabolic mirror.

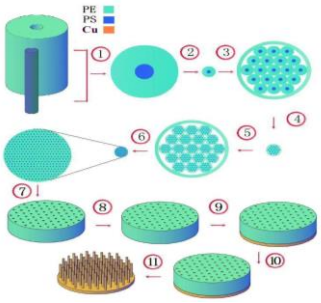

Fig. 1. A schematic illustrations of Cu nanowire arrays fabrication using iterative melt bundling co-drawing and electrodeposition with eleven key steps: 1) insetting PS rod to PE tube to make a preformed rod, 2) reducing the diameter of PS rod by melt co-drawing first time, 3) bundling the reduced rod with PE tube first time, 4) reducing the diameter of PS rod by melt co-drawing second time, 5) bundling the reduced rod with PE tube second time, 6) reducing the diameter of PS rod by melt co-drawing third time, 7) cutting a segment of the PE/PS rod, 8) dissolving PS and getting a PE template with nanohole arrays, 9) sputtering a Cu film to one side of the template, 10) electrodepositting Cu in the nanohole arrays, 11) dissolving PE and getting Cu nanowire arrays

3. Results and discussion

Fig. 2 shows scanning electron microscopy (SEM) images of [(a) and (c)] PE templates with micro/nanopore arrays and corresponding side-view images of [(b) and (d)] Cu micro/nanowire arrays. High precision hexagonal packing of micropores in PE matrix is shown in Fig. 2a, in which 84% pores are found to be 3.5 μm and the spacings about 40 μm. This image was taken at the cross section of the fiber obtained from the second melt co-drawing step. PS fibers embedded in PE were selectively removed by immersing the sample in methylbenzene solution and the pore arrays were well conserved. Based on this PE templates, Cu microwire arrays were fabricated by sputtering a Cu film, electrodeposition Cu microwire and selectively dissolving PE, the side-view SEM image of Cu microwire arrays was shown in Fig. 2b. The diameters of the obtained microwires are about 3.5 μm, the length about 30 μm and the spacings about 40 μm, which are in accordance with the size of the template shown in Fig. 2a. The drawing step was repeated a third time, the micrometersized fibres obtained from the previous step will become nanometresized wires, and the results are shown in Fig. 2c and Fig. 2d. The diameters of the obtained nanowires are about 200 nm, the length about 1.5 μm and the spacings about 2μm. To demonstrate the controllability of our method, another series of experiments should been performed in the future.

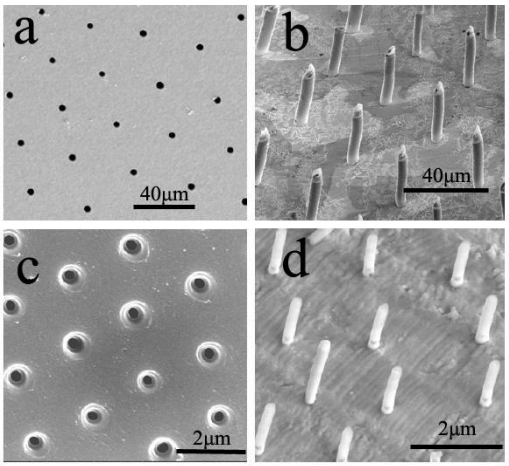

Fig. 2. Scanning electron microscopy (SEM) images of [(a) and (c)] PE templates with micro/nanopore arrays and corresponding [(b) and (d)] Cu micro/nanowire arrays

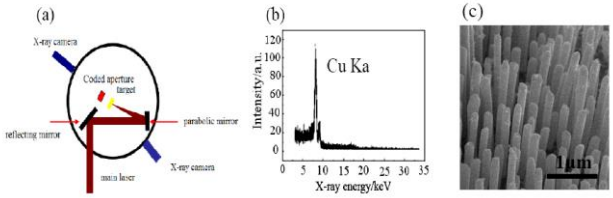

Fig. 3. Schematic overview of the experimental setup (a), a typical x-ray energy spectrum observed in the experiments (b), and SEM image of Cu nanowire arrays (c)

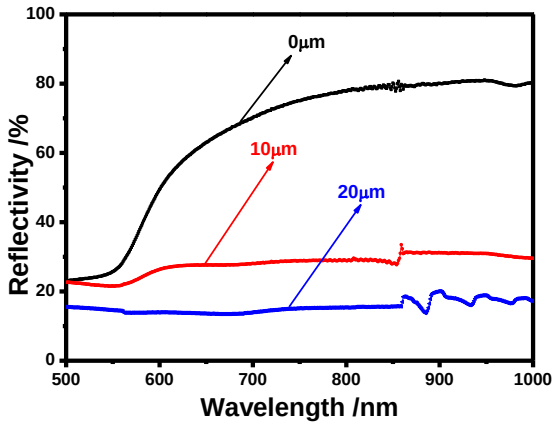

Fig. 4. Reflectivity of Cu nanowire arrays with different nanowire length. The light wavelength is 500nm~1000nm. The diameter of the individual fibers is about 200 nm and the spacing between them is about 150 nm. The length of nanowire arrays are 0μm(planar Cu), 10 μm and 20 μm, respectively

Finally, we investigated the interaction between intense ultrashort pulse laser and solid targets. Cu nanowire arrays fabricated using the described technique and planar Cu were employed. The SEM image of the Cu nanowire arrays target is shown in Fig. 3c. The diameter of the individual fibers is about 200 nm, the mean length of nanowire arrays is about 20μm and the spacing between them is about 150 nm. The experimental setup is shown in Fig. 3a. The laser can deliver energies up to 6 J (with a peak intensity of 7.9×10^{18} W cm^{-2}), the pulse duration is 31 fs, and the central wavelength is 800 nm. After entering the chamber, the *p*-polarized main laser is focused on the target with an *f* /3 off-axis-parabolic mirror. Fig. 3b shows a measured x-ray energy spectrum with a typical Kα line near 8 keV for a nanowire arrays copper target. Three times enhancement (from that for a planar target) in the x-ray yield is observed. [12] That is, a nanowire arrays target can significantly enhance the hot electron number as well as energy. G. Kulcsár attribute the x-ray yield increase from the structured targets to at least three factors. [11] First, structuring the target surface significantly enhances the light absorption for the nanowires which appears nearly black in visible light. Fig. 4 shows the reflectivity of Cu nanowire arrays with different nanowire length. The reflectivity of Cu nanowire arrays are 77.9%, 28.8% and 15.4% for 800 nm laser wavelength, and the corresponding nanowire length are 0 μm (planar Cu), 10 μm and 20 μm. The reflectivity is observed to decrease with increaseing of nanowire length. Second, even after plasma formation the critical density surface of the target will be deeply convoluted, being positioned at the cylindrically expanding plasma around the nanowires, thus maintaining a large absorption coefficient in the high-intensity regime—an effect greatly exaggerating that of absorption increase by critical-surface rippling. Third, because of the low average density and high local density of the micro/nanowire arrays targets, the laser will heat or ablate about a 17 fold depth than the optical coupling depth (skin depth) of solid material to the point of producing soft x rays. Therefore, in the velvet target a depth of many more metal atoms are heated, and so the temperature scale-length is also longer—both in laboratory coordinates and as indexed by areal density of material.

4. Conclusions

In summary, an effective and simple method for mass production of metallic micro/nanowire arrays has been demonstrated. In this approach, the three dimensional geometric parameters of the metallic array can be tuned over a large range, from micron- to nano-scale, using porous PE templates basing on iterative melt codrawing and bundling technique. Plasmas created by the interaction of intense femtosecond laser pulses with matter offer new opportunities for both studying high-energy-density physics and designing novel sources of femtosecond X-ray, electron and ion pulses. [28,29] Metallic micro/nanowire arrays with largely tunable diameter and spacing can be used as velvet targets, and the obtained X-ray-flux gain of more than 50 in the ~1 keV energy region using vertically aligned metallic nanowire arrays suggests that it may be possible to generate high-flux, short-pulse, compact X-ray sources based on Cu, Ni and Au micro/nanowire arrays.

Acknowledgements

Niu Gao and Yang Bo contributed equally to this work. We thank the LFRC staff for the laser operation, and data acquisition. This work is supported by the Foundation of Science and Technology on Plasma Physics Laboratory (9140C680502120C68255), the Natural Science Foundation of China (11135007 and 11204280), the Foundation of Precision Manufacturing Technology, CAEP (ZZ14010).

References

[1] R. B. Stephens, R. A. Snavely, Y. Aglitskiy, F. Amiranoff, C. Andersen, D. Batani, S. D. Baton, T. Cowan, R. R. Freeman, T. Hall, S. P. Hatchett, J. M. Hill, M. H. Key, J. A. King, J. A. Koch, M. Koenig, A. J. MacKinnon, K. L. Lancaster, E. Martinolli, P. Norreys, E. Perelli-Cippo, M. Rabec Le Gloahec, C. Rousseaux, J. J. Santos, F. Scianitti, Phys. Rev. E **69**, 066414 (2004).

[2] V. I. Eremin, A. V. Korzhimanov, A. V. Kim, Phys. Plasmas **17**, 043102 (2010).

[3] S. Kar, A. P. L. Robinson, D. C. Carroll, O. Lundh, K. Markey, P. McKenna, P. Morreys, M. Zepf, Phys. Rev. Lett. **102**, 055001 (2009).

[4] H. Nakamura, B. Chrisman, T. Tanimoto, M. Borghesi, K. Kondo, M. Nakatsutsumi, T. Norimatsu, M. Tampo, K. A. Tanaka, T. Yabuuchi, Y. Sentoku, R. Kodama, Phys. Rev. Lett. **102**, 045009 (2009).

[5] J. Fuchs, P. Antici, E. D'Humières, E. Lefebvre, M. Borghesi, E. Brambrink, C. A. Cecchetti, M. Kaluza,

V. Malka, M. Manclossi, S. Meyroneinc, P. Mora, J. Schreiber, T. Toncian, H. Pépin, Nat. Phys. **2**, 48 (2006).
[6] S. Ter-Avetisyan, M. Schnürer, P. V. Nickles, W. Sandner, M. Borghesi, T. Nakamura, K. Mima, Phys. Plasmas **17**, 063101 (2010).
[7] A. Rousse, C. Rischel, J.-C. Gauthier, Rev. Mod. Phys. **73**, 17 (2001).
[8] L. M. Chen, F. Liu, W. M. Wang, M. Kando, J. Y. Mao, L. Zhang, J. L. Ma, Y. T. Li, S. V. Balanov, T. Tajima, T. Kato, Z. M. Sheng, Z. Y. Wei, J. Zhang, Phys. Rev. Lett. **104**, 215004 (2010).
[9] U. Teubner, P. Gibbon, Rev. Mod. Phys. **81**, 445 (2009).
[10] M. Tabak, J. Hammer, M. E. Glinsky, W. L. Kruer, S. C. Wilks, J. Woodworth, E. M. Campbell, M. D. Perry, R. J. Mason, Phys. Plasmas **1**, 1626 (1994).
[11] G. Kulcsár, D. Mawlawi, F. Budnik, P. Herman, M. Moskovits, L. Zhao, R. Marjoribanks, Phys. Rev. Lett. **84**, 5149 (2000).
[12] Z. Zhao, L. Cao, L. Cao, Phys. Plasmas.**17**, 123108 (2010).
[13] L. Cao, Y. Gu, Z. Zhao, L. Cao, W. Huang, W. Zhou, X. He, W. Yu, M. Yu, Phys. Plasmas. **17**, 043103 (2010).
[14] Z. F. Ren, Z. P. Huang, J. W. Xu, J. H. Wang, P. Bush, M. P. Siegal, P. N. Provencio, Science, **282**, 1105 (1998).
[15] L. M. Huang, H. T. Wang, Z. B. Wang, A. Mitra, K. N. Bozhilov, Y. S. Yan, Adv. Mater., **14**, 61 (2002).
[16] H. Yoon, D. C. Deshpande, V. Ramachandran, V. K. Varadan, Nanotechnology, **19**, 025304 (2008).
[17] W. Y. Yuan, Z. S. Lu, J. P. Liu, H. L. Wang, C. M. Li, Nanotechnology, **24**, 045605 (2013).
[18] Y. Chen, L. N. Zhang, X. Y. Lu, N. Zhao, J. Xu, Macromol. Mater. Eng., **291**, 1098 (2006).
[19] Y. C. Xie, Y. Xu, K. L. Yung, Polym. Eng. Sci., **52**, 205 (2012).
[20] W. Lee, R. Ji, U. Gosele, K. Nielsch, Nature Mater., **5**, 741 (2006).
[21] Q. Zhao, G. H. Wen, Z. G. Liu, Y. B. Fan, G. T. Zou, L. Li, R. K. Zheng, S. P. Ringer, H. K. Mao, Nanotechnology, **22**, 125603 (2011).
[22] T. Han, P. Y. Wen, C. Y. Wang, X. F. Zhu, Mater. Rev., **24**, 115 (2010).
[23] X. Ye, X. D Jiang, J. Huang, F. Geng, L. X. Sun, X. T. Zu, W. D. Wu, W. G. Zheng, Sci. Rep. **5**, 13023 (2015).
[24] X. Ye, J. Huang, R.F. Ni, Z. Yi, X. D. Jiang, W. G. Zheng, J. Optoelectron. Adv. Mater.**17**, 192 (2015).
[25] X. Ye, J. Huang, J. C. Zhang, X. D. Jiang, W. D. Wu, W. G. Zheng, J. Optoelectron. Adv. Mater. **13**, 532 (2011).
[26] B. Yang, G. Niu, X. Zhou, X. Liu, W. He, B. Yu, Y. Zhu, W. Wu, Polym. Engin. Sci. 2014, DOI 10.1002/pen.23997.
[27] M. Yaman, T. Khudiyev, E. Ozgur, M. Kanik, O. Aktas, E. O. Ozgur, H. Deniz, E. Korkut, M. Bayindir, Nat. Mater. **10**, 494 (2011).
[28] L. V. Dao, P. Hannaford, Nature Photon. **7**, 771 (2013).
[29] M. A. Purvis1, V. N. Shlyaptsev, R. Hollinger, C. Bargsten1, A. Pukhov, A. Prieto, Y. Wang, B. M. Luther, L. Yin, S. Wang, J. J. Rocca, Nature Photon. **7**, 796 (2013).

*Corresponding author: xiuwenzhou@caep.cn